9 Monte Carlo renormalization group methods

9.1 INTRODUCTION TO RENORMALIZATION GROUP THEORY

The concepts of scaling and universality presented in the second chapter of this book can be given concrete foundation through the use of renormalization group (RG) theory. The fundamental physical ideas underlying RG theory were introduced by Kadanoff (1971) in terms of a simple coarse-graining approach, and a mathematical basis for this viewpoint was completed by Wilson (1971). Kadanoff divided the system up into cells of characteristic size ba, where a is the nearest neighbor spacing, and $ba < \xi$, where ξ is the correlation length of the system (see Fig. 9.1). The singular part of the free energy of the system can then be expressed in terms of cell variables instead of the original site variables, i.e.

$$F_{\text{cell}}(\tilde{\varepsilon}, \tilde{H}) = b^d F_{\text{site}}(\varepsilon, H), \tag{9.1}$$

where $\varepsilon = |1 - T/T_c|$, $\tilde{\varepsilon}$ and $\tilde{H}$ are cell variables, and d is the lattice dimensionality. This is merely a statement of the homogeneity of the free energy and yields the scaling expression

$$F(\lambda^{a_T}\varepsilon, \lambda^{a_H} H) = \lambda F(\varepsilon, H). \tag{9.2}$$

According to formal RG theory the initial Hamiltonian is transformed, or *renormalized* to produce a new Hamiltonian; this process may be repeated many times and the resultant Hamiltonians, which may be given a characteristic index n to describe the number of times the transformation has been applied, are related by

$$\mathcal{H}^{(n+1)} = \boldsymbol{R}_b \mathcal{H}^{(n)}. \tag{9.3}$$

The renormalization group operator $\boldsymbol{R}_b$ acts to reduce the number of degrees of freedom by b^d where b is the spatial rescaling factor and d the spatial dimensionality. (It is perhaps worthwhile pointing out that this generally does not constitute a true group theory since $\boldsymbol{R}_b$ typically has no inverse.) Note that the renormalized Hamiltonian may contain terms (i.e. additional couplings) which were not originally present and which appear only as a result of the renormalization transformation. Of course, the partition function Z must not be changed by this process since it is only being expressed in terms of new

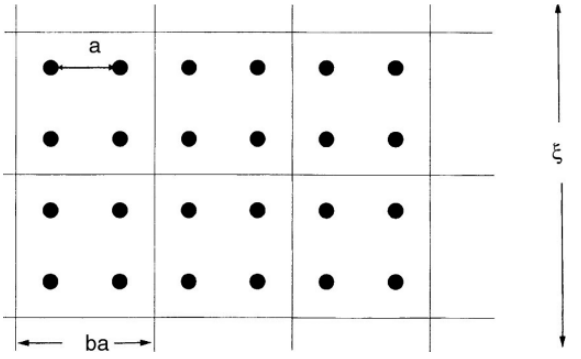

Fig. 9.1 Schematic subdivision of the lattice into cells. The lattice constant is a, the rescaling factor is b, and the correlation length is denoted as ξ.

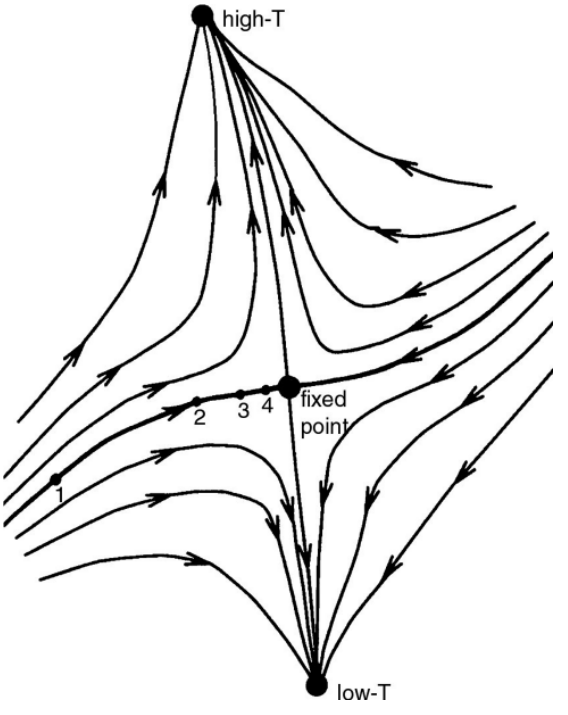

Fig. 9.2 Schematic RG flow diagram in a two-dimensional parameter space. The heavy curve represents the critical hypersurface. Point 1 is the critical value and the other points labeled show the flow towards the fixed point (heavy filled circle).

variables. After the transformation has been applied many times the Hamiltonian has reached an invariant or 'fixed point' form $\mathcal{H}^*$ and no longer changes, i.e.

$$\mathcal{H}^* = \boldsymbol{R}_b \mathcal{H}^*. \tag{9.4}$$

This means that the Hamiltonian of a system at its critical point will move, or 'flow', *towards* the fixed point Hamiltonian upon successive applications of the RG transformation until the form no longer changes. Conversely, if the system is not initially at a critical point, upon renormalization the Hamiltonian will 'flow' *away* from the fixed point of interest (see Fig. 9.2). In a study of an Ising-type Hamiltonian for $T > T_c$ one ultimately reaches a trivial fixed

point corresponding to the ideal paramagnet at $T \to \infty$. (After a few rescalings the block size ab^n exceeds ξ and the different blocks are then uncorrelated.) For $T < T_c$ the flow is to a different, zero temperature fixed point. The Hamiltonian is written in the same general framework at each application of the transformation, e.g. an Ising-type Hamiltonian

$$\mathcal{H}/k_B T = K_1 \sum_i S_i + K_2 \sum_{\langle i,j \rangle} S_i S_j + K_3 \sum_{\langle i,j,k \rangle} S_i S_j S_k + K_4 \sum_{\langle i,j,k.l \rangle} S_i S_j S_k S_l + \cdots . \tag{9.5}$$

The space of coupling constants $\{K_1, K_2, \ldots\}$ is then the space in which the flow is considered. A model Hamiltonian can generally be extended to include other interactions such that an entire hypersurface of critical points is produced; in all cases in which we begin on the critical hypersurface, the system Hamiltonian should move, or 'flow', towards the fixed point of interest. When a system is at a multicritical point, it will flow towards a new 'fixed point' instead of towards the critical fixed point. Close to the multicritical point there may be complex crossover behavior and the system may at first appear to flow towards one fixed point, but upon further application of the RG transformation it begins to flow towards a different fixed point. Thus, RG theory very nicely illuminates the universality principle of critical phenomena: each type of criticality is controlled by a particular fixed point of the RG transformation that is considered (Fisher, 1974a).

Near the fixed point one can generally linearize the problem so that the Hamiltonian $\mathcal{H}'$ is related to the fixed point form by

$$\mathcal{H}' = \boldsymbol{R}_b[\mathcal{H}^*] + h\boldsymbol{L}\underline{Q} = \mathcal{H}^* + h\boldsymbol{L}\underline{Q} + \cdots , \tag{9.6}$$

where the linear operator $\boldsymbol{L}$ has the eigenvalue equation

$$\boldsymbol{L}\underline{Q}_j = \lambda_j \underline{Q}_j \tag{9.7}$$

with λ_j being the eigenvalue and $\underline{Q}_j$ the eigenvector. In terms of the spatial rescaling factor b

$$\lambda_j = b^{y_j}, \tag{9.8}$$

where y_j is termed an 'exponent eigenvalue' which can be related to the usual critical exponents, as we shall see later. We can then write an expression for the transformed Hamiltonian in terms of these eigenvalues

$$\mathcal{H}' = \mathcal{H}^* + \sum h_j \lambda_j \underline{Q}_j + \cdots . \tag{9.9}$$

From this equation we can immediately write down recursion relations for the h_j

$$h_j^{(k+1)} \approx \lambda_j h_j^{(k)} \tag{9.10}$$

which may be solved to give values for the eigenvalues. The singular part of the free energy in terms of the original and renormalized variables is again unchanged:

$$f(h_1, h_2, h_3, \ldots) \approx b^{-d} f(b^{\lambda_1} h_1, b^{\lambda_2} h_2, \ldots) \tag{9.11}$$

where we may identify $h_1 = k_1 t$, $h_2 = k_2 H$, etc. We have redefined $|1 - T/T_c|$ as t in order to reserve the symbol ε for $4 - d$ in keeping with the standard notation in renormalization group theory (see below). Choosing b so that $b^{\lambda_1} t = 1$, we can rewrite this equation with k_1, k_2 constants

$$f(t, H, h_3) \approx t^{d/\lambda_1} f(k_1, k_2, H/t^{\lambda_2/\lambda_1}, \ldots). \tag{9.12}$$

Thus, if we identify $d/\lambda_1 = 2 - \alpha$ and $\lambda_2/\lambda_1 = \Delta$, we have 'derived' scaling.

For completeness, we briefly mention the momentum space approach to renormalization group theory. In this case the coarse-graining and rescaling which occurs as part of the RG process is defined in k-space (momentum space instead of real space). In terms of a Landau-like Hamiltonian, the Fourier space form is

$$\mathcal{H}(m) = 1/2 \int k^{d-1} dk (k^2 + r_o) |m(k)|^2 + \cdots. \tag{9.13}$$

A cutoff momentum Λ is then introduced, the k values which lie between Λ and Λ/b are integrated out, and then the variable of integration is rescaled by $k' = bk$. The order parameter is then renormalized and one subsequently repeats the same steps. A perturbation expansion is then realized which leads to recursion relations for the effective interaction parameters. The solution to these equations gives rise to the 'fixed points' in the problem. Perturbation parameters may include the difference in lattice dimensionality from the upper critical dimension $\varepsilon = (d_u - d)$ or the inverse of the number of components of the order parameter n. For simple magnetic systems with isotropic, short range couplings the upper critical dimension is $d_u = 4$ and the leading order estimates for critical exponents are (Wilson and Fisher, 1972):

$$\alpha = \frac{4 - n}{2(n + 8)} \varepsilon + \cdots \qquad \text{where } \varepsilon = 4 - d, \tag{9.14a}$$

$$\beta = \frac{1}{2} - \frac{3}{2(n + 8)} \varepsilon + \cdots, \tag{9.14b}$$

$$\gamma = 1 + \frac{(n + 2)}{2(n + 8)} \varepsilon + \cdots. \tag{9.14c}$$

Of course, for simple models of statistical mechanics higher order expressions have been derived with the consequence that rather accurate estimates for critical exponents have been extracted, see e.g. Brezin *et al.* (1973) and Zinn-Justin and Le Guillou (1980). A rather sophisticated analysis of the expansions is required in general. Renormalization group theory was used to successfully understand the behavior of the tricritical point by Wegner and Riedel (1973)

who showed that Landau theory exponents are indeed correct in three dimensions but that the critical behavior is modified by the presence of logarithmic corrections. Further, a renormalization group analysis of bicritical and related tetracritical points has been carried out by Nelson *et al.* (1974). While the momentum space RG has yielded fairly accurate results for the critical exponents of the n-vector model, the accuracy that was reached for other problems is far more modest, e.g. universal scaling functions describing the equation of state, or describing the crossover from one universality class to another, typically are available in low order ε-expansion only, and hence describe real systems qualitatively but not quantitatively. Moreover, the momentum space RG in principle yields information on universal properties only, but neither information on the critical coupling constants (T_c, etc.) nor on critical amplitudes (Chapter 2) is provided. The real space RG can yield this information, and hence we turn to this approach now. This work has been augmented by Monte Carlo simulations which have examined tricritical behavior in the three-dimensional Ising model and explored the four-dimensional phase diagram, i.e. in $H_\parallel$, $H_\perp$, $H_{||}^+$, T space, of the anisotropic Heisenberg model.

Of course, RG theory is a huge subject with many subtle aspects which can fill volumes (e.g. Domb and Green, 1976). Here we only wish to convey the flavor of the approach to the reader and emphasize those aspects which are absolutely indispensible for understanding the literature which uses Monte Carlo renormalization group methods.

9.2 REAL SPACE RENORMALIZATION GROUP

A number of simple RG transformations have been used with generally good success. By 'simple' we mean that the space of coupling constants that is allowed for is kept low-dimensional: this is an arbitrary and uncontrolled approximation, but it allows us to carry out the calculations needed for the renormalization transformation in a fast and convenient way. One approach is the 'blockspin' transformation in which a $b \times b$ block of spins is replaced by a 'superspin' whose state is determined by the state of the majority of spins in the block. If the number of spins in a block is even, one site in each block is designated as a 'tie-breaker'. Another alternative is the 'decimation' process in which the lattice is renormalized by taking every bth spin in all directions. In a nearest neighbor antiferromagnet a simple majority rule over a 2×2 blockspin would give zero for all blockspins when the system was in the groundstate. Thus a more natural and useful choice is to have the 'blockspins' composed of more complex structures where each block resides on a single sublattice. Examples of several blockspin choices are shown in Fig. 9.3. Note that the $\sqrt{5} \times \sqrt{5}$ transformation rotates the lattice through an angle $\varphi = \pi/4$ (this rotation effect is shown more clearly for the $\sqrt{7} \times \sqrt{7}$ transformation on the right in Fig. 9.3) but preserves the square lattice symmetry. If a second transformation is applied but chosen to rotate the lattice through angle $-\varphi$ the original orientation is recovered. The underlying ideas of RG theory are demonstrated in

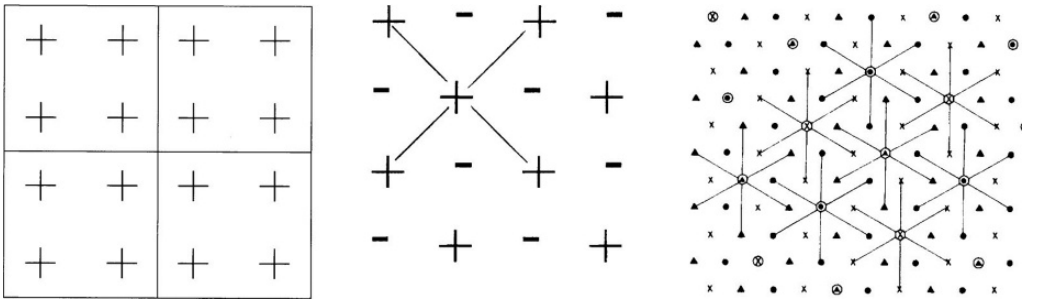

Fig. 9.3 Examples of simple blockspins: (left) (2 × 2) blockspin arrangement for a ferromagnet; (center) $\sqrt{5} \times \sqrt{5}$ blockspin for a nearest neighbor antiferromagnet in which each spin in a blockspin is on the same sublattice; (right) $\sqrt{7} \times \sqrt{7}$ blockspin for a nearest neighbor antiferromagnet on a triangular lattice in which each spin in a blockspin is on the same sublattice.

Fig. 9.4 where we have taken Monte Carlo generated configurations in a spin-$\frac{1}{2}$ Ising model on a 512 × 512 square lattice with periodic boundaries at three different temperatures near T_c. A $b = 2$ blockspin transformation is applied and then the lattice is rescaled to the original size. At $0.95T_c$ the system rapidly becomes almost completely ordered under application of the RG transformation. At T_c the system is virtually invariant with successive application of the transformation. Since the initial lattice was finite there is still a finite size effect and the total magnetization is not zero for this particular configuration. At $1.05T_c$ the system is disordered and the renormalized magnetization becomes even smaller. As for the rescaling transformation in Eqn. (9.3), if one could carry this out exactly an increasing number of couplings $\{K_i\}$ in a Hamiltonian like Eqn. (9.5) would be generated. However, in practice, as the rescaling is iterated the space of coupling constants has to be truncated dramatically, and in an analytic approach other uncontrolled approximations may be necessary to relate the new couplings to the old couplings. These latter problems can be avoided with the help of Monte Carlo renormalization group methods which we wish to describe here.

9.3 MONTE CARLO RENORMALIZATION GROUP

9.3.1 Large cell renormalization

The large cell renormalization group transformation was used to study both spin systems (Friedman and Felsteiner, 1977; Lewis, 1977) and the percolation problem (Reynolds *et al.*, 1980). In this discussion we shall consider the method in the context of the two-dimensional Ising model with nearest neighbor coupling only. A system of size $L \times 2L$ is considered and two blockspins, σ_1' and σ_2', are created from application of the majority rule to 'large' cells of size $L \times L$. The blockspins interact with Hamiltonian

$$\mathcal{H} = K'\sigma_1'\sigma_2', \tag{9.15}$$

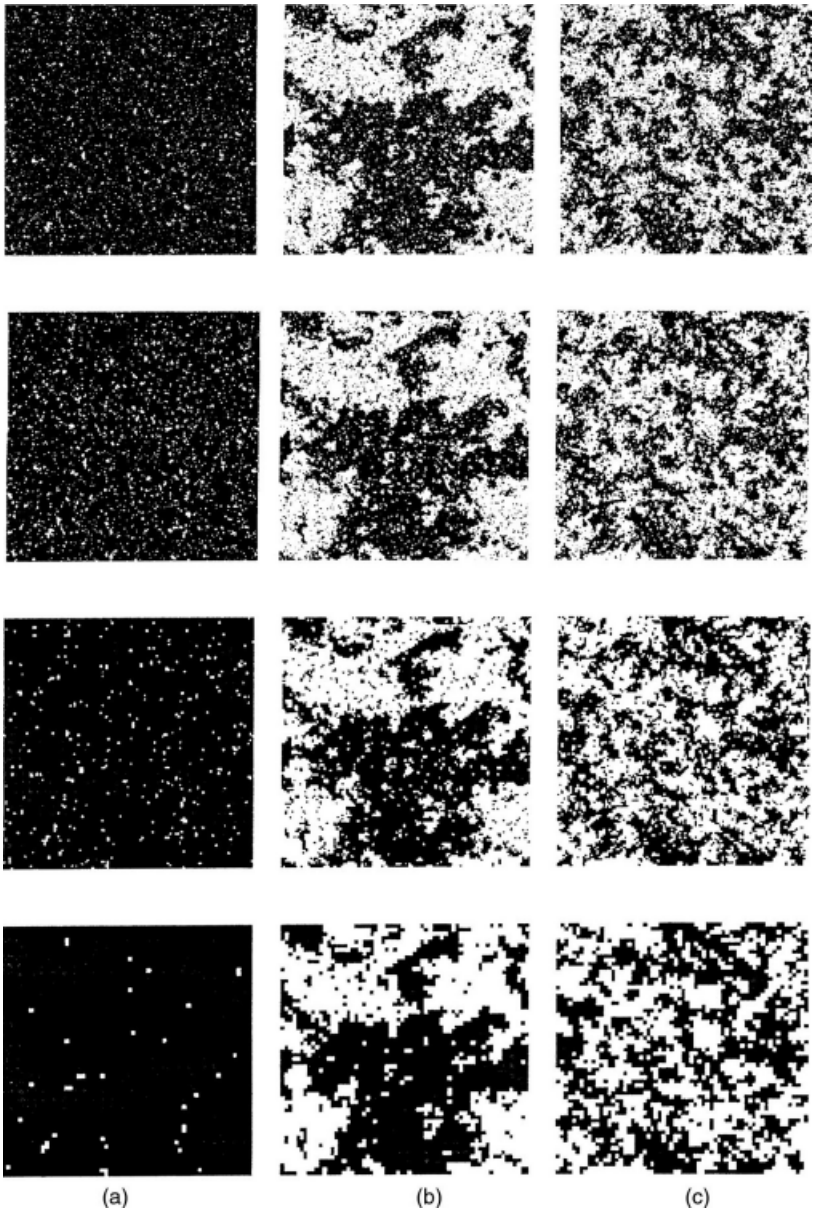

Fig. 9.4 'Snapshots' of the two-dimensional Ising model at: (a) $T = 0.95\ T_c$; (b) $T = T_c$; (c) $T = 1.05\ T_c$. The upper row shows Monte Carlo generated configurations on a 512×512 lattice with periodic boundaries. Successive rows show the configurations after 2×2 blockspin transformations have been applied and the lattices rescaled to their original size.

where the magnitude of the new effective coupling constant K' is determined from

$$\sigma_1'\sigma_2' = \tanh(q\,K'). \tag{9.16}$$

Note that this corresponds to a transformation with scale factor $b = L$. The thermal eigenvalue y_T is then determined from the expression

$$\frac{d\,K'}{d\,K} = L^{y_T}, \tag{9.17}$$

where the derivative can be calculated via Monte Carlo simulation from averages, i.e.

$$\frac{dK'}{dK} = \langle \sigma_1' \sigma_2' S_1 \rangle - \langle \sigma_1' \sigma_2' \rangle \langle S_1 \rangle. \tag{9.18}$$

If L is increased with the system held at the critical coupling the estimates for y_T should converge to the correct value of $1/\nu$.

Problem 9.1 Simulate a 16 × 32 Ising square lattice at T_c and use the large cell Monte Carlo renormalization method to estimate the value of the thermal exponent y_T.

9.3.2 Ma's method: finding critical exponents and the fixed point Hamiltonian

The Monte Carlo method was first used within the framework of renormalization group theory by Ma (1976) who applied it to the study of critical exponents in a simple Ising model system. The basic idea of this approach is to determine the behavior of the Hamiltonian upon renormalization and by following the 'flow' towards the fixed point Hamiltonian to study critical exponents. By measuring effective interaction parameters between coarse-grained blocks of spins, one can extract exponent estimates from this information. The method begins by generating a sequence of states. 'Probes' of different sizes are then used to measure interactions by observing how a spin behaves in a given environment. The length of time it takes for a spin to flip in a given environment is a reflection of the interaction parameters as well as the 'local' structure, and by examining different local environments one can produce a set of linear equations that may be solved for the individual interaction constants. This process may be repeated by examining the behavior of blockspins, i.e. of a 2 × 2 set of spins whose blockspin value is chosen to be $\tilde{S} = 1$ if a majority of the spins in the block are 1s and $\tilde{S} = -1$ if the majority are –1s. Applying the same procedure outlined above provides a set of interaction parameters at a scale which is twice as large as that defined by the small probe.

The actual implementation demonstrated by Ma was for the Ising model with a set of interaction parameters $\mu = (\mathcal{J}, K, L)$ which represent nearest neighbor, next-nearest neighbor, and four-spin interaction parameters and has much of the flavor of the N-fold way algorithm. The rate of flipping for each spin is determined in the following way. The probability that no spin-flips during the time period t' (the 'lifetime' of the state) is $\exp(-\Omega t')$ where Ω is the total transition rate for the entire system. The probability that no spin-flips in the initial interval but then flips in the following dt' interval is $\exp(-\Omega t') \times dt'$. The lifetime for a given spin is determined by generating one random number to select a spin and then a second random number x to determine the lifetime through $t' = -(\ln x)/\Omega$. The small probe looks at 3 × 3 blocks of spins and determines τ_+ and τ_-, i.e. the lifetimes of the states where the spin is +1 and –1 respectively. The ratio $\tau_+/\tau_- = \exp(\mathcal{H} - \mathcal{H}')$ gives an

equation for $\mathcal{J}$, K, and L. (For example, if all the spins in the probe are $+1$, then $(\mathcal{H} - \mathcal{H}') = 4(\mathcal{J} + K + L)$.) If the ratio of lifetimes is measured for three different neighbor environments, a set of linear equations is obtained which can be solved to extract each individual interaction parameter. To determine the critical exponent we want to repeat this procedure with the large probe and then construct the matrix $(\partial \mathcal{J}_i'/\partial \mathcal{J}_i)$, the largest eigenvalue of which is $\lambda_T = 2^{1/\nu}$. Unfortunately, in actual practice it proves quite difficult to determine the fixed point Hamiltonian with significant accuracy.

9.3.3 Swendsen's method

Ma's method proved difficult to implement with high accuracy because it was very difficult to calculate the renormalized Hamiltonian accurately enough. A very different approach, which is outlined below, proved to be more effective in finding exponent estimates because it is never necessary to calculate the renormalized couplings. For simplicity, in the discussion in this subsection we shall express the Hamiltonian in the form

$$\mathcal{H} = \sum_{\alpha} K_\alpha S_\alpha, \tag{9.19}$$

where the S_α are sums of products of spin operators and the K_α are the corresponding dimensionless coupling constants with factors of $-1/kT$ absorbed. Examples of spin products are:

$$S_1 = \sum \sigma_i, \tag{9.20a}$$

$$S_2 = \sum \sigma_i \sigma_j, \tag{9.20b}$$

$$S_3 = \sum \sigma_i \sigma_j \sigma_k. \tag{9.20c}$$

Near the fixed point Hamiltonian $\mathcal{H}^*(K^*)$ the linearized transformation takes the form

$$K_\alpha^{(n+1)} - K_\alpha^* = \sum_{\beta} T_{\alpha\beta}^* \left(K_\beta^{(n)} - K_\beta^*\right), \tag{9.21}$$

where the sum is over all possible couplings. The eigenvalues λ_i of $T_{\alpha\beta}^*$ are related to eigenvalue exponents by

$$\lambda = b^y, \tag{9.22}$$

where the y are in turn related to the usual critical exponents, e.g. $y_T = \nu^{-1}$.

Equations (9.21) and (9.22) are still common to all real space RG methods, and the challenge becomes how to find the matrix elements $T_{\alpha\beta}^*$ at the fixed point in practice. Perhaps the most accurate implementation of real space RG methods has been through the use of Monte Carlo renormalization group (MCRG) methods (Swendsen, 1982). In this approach the elements of the

Table 9.1 *Variation of the thermal eigenvalue exponent for the Ising square lattice with the number of couplings N_c, the number of iterations N_r, and for different lattice sizes. From Swendsen (1982).*

N_r	N_c	$L = 64$	$L = 32$	$L = 16$
1	1	0.912(2)	0.904(1)	0.897(3)
1	2	0.967(3)	0.966(2)	0.964(3)
1	3	0.968(2)	0.968(2)	0.966(3)
1	4	0.969(4)	0.968(2)	0.966(3)
2	1	0.963(4)	0.953(2)	0.937(3)
2	2	0.999(4)	0.998(2)	0.993(3)
2	3	1.001(4)	1.000(2)	0.994(3)
2	4	1.002(5)	0.998(2)	0.984(4)
3	1	0.957(2)	0.936(3)	0.921(5)
3	2	0.998(2)	0.991(3)	1.013(4)
3	3	0.999(2)	0.993(3)	1.020(3)
3	4	0.997(2)	0.987(4)	...

linearized transformation matrix are written in terms of expectation values of correlation functions at different levels of renormalization. Thus,

$$T_{\alpha\beta} = \frac{\partial K_\alpha^{(n+1)}}{\partial K_\beta^{(n)}}, \tag{9.23}$$

where the elements can be extracted from solution of the chain rule equation

$$\partial \langle S_\gamma^{(n+1)} \rangle / \partial K_\beta^{(n)} = \sum \{ \partial K_\alpha^{(n+1)} / \partial K_\beta^{(n)} \} \{ \partial \langle S_\gamma^{(n+1)} \rangle / \partial K_\alpha^{(n+1)} \} . \tag{9.24}$$

The derivatives can be obtained from correlation functions which can be evaluated by Monte Carlo simulation, i.e.

$$\partial \langle S_\gamma^{(n+1)} \rangle / \partial K_\beta^{(n)} = \langle S_\gamma^{(n+1)} S_\beta^{(n)} \rangle - \langle S_\gamma^{(n+1)} \rangle \langle S_\beta^{(n)} \rangle \tag{9.25}$$

and

$$\partial \langle S_\gamma^{(n)} \rangle / \partial K_\alpha^{(n)} = \langle S_\gamma^{(n)} S_\alpha^{(n)} \rangle - \langle S_\gamma^{(n)} \rangle \langle S_\alpha^{(n)} \rangle . \tag{9.26}$$

The $T_{\alpha\beta}$ matrix is truncated in actual calculations and the number of renormalizations is, of course, limited as well. Results for the estimates for eigenvalues are then examined as a function of the number of couplings N_c used in the analysis and the number of iterations N_r. Exact results are expected only for $N_r \to \infty$ and $N_c \to \infty$, but in practice the convergence to this limit is rather fast. By performing the calculations on different size lattices one can also determine if finite-lattice size is playing a role. As a simple example, in Table 9.1 we show data for the thermal eigenvalue exponent for $L \times L$ square lattice Ising models. As the number of iterations increases the exponent rapidly converges

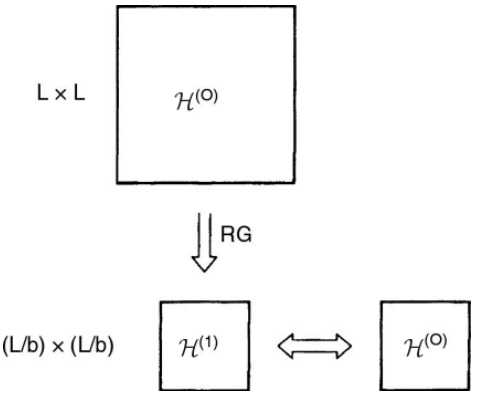

Fig. 9.5 Schematic view of the two lattice comparison for the determination of the critical temperature.

to the exact value $y_T = 1.0$, but this is true only as long as at least one additional coupling is generated. Finite size effects also begin to appear slowly and become increasingly important as the iteration number increases.

Experience with other models has shown that in general the convergence is not as rapid as for the two-dimensional Ising model and great care must be used to insure that a sufficient number of couplings and renormalizations have been used. This also means, of course, that often rather large lattices must be used to avoid finite size effects in the renormalized systems.

There have not been any substantive methodological improvements over the past few years; nevertheless, the method has its place among other simulation methods for the study of critical behavior. See, for example, Itakura (2002), Hsiao and Monceau (2003), and Guo *et al.* (2005).

Problem 9.2 Simulate a 27×27 Ising square lattice ferromagnet at T_c and use Swendsen's method with $b = 3$ to estimate the thermal exponent y_T.

9.3.4 Location of phase boundaries

9.3.4.1 Critical points

How do we determine the location of the critical point using the ideas of MCRG? This may be accomplished by matching correlation functions for transformed and untransformed systems: only at the critical point will they be the same. Finite size effects can be subtle, however, so the preferred procedure is to start with two different lattices which differ in size by the scale factor b to be used in the transformation (see Fig. 9.5). In the vicinity of the critical point we can use a linear approximation to relate the difference between the original and renormalized correlation functions to the distance to the critical point, i.e.

$$\left\langle S_\alpha^{(n)} \right\rangle_L - \left\langle S_\alpha^{(n-1)} \right\rangle_S = \sum_\beta \left[\frac{\partial \left\langle S_\alpha^{(n)} \right\rangle_L}{\partial K_\beta^{(0)}} - \frac{\partial \left\langle S_\alpha^{(n-1)} \right\rangle_S}{\partial K_\beta^{(0)}} \right] \delta K_\beta^{(0)}. \quad (9.27)$$

The predicted 'distance' from the critical coupling $\delta K_\beta^{(0)}$ can be extracted by inverting Eqn. (9.27) for different values of n. Thus, an initial estimate for the critical coupling is chosen and the above process is carried out. The simulation is then repeated at the updated estimate and a check is made to see if this is, in fact, a good value.

9.3.4.2 Multicritical points

The methods described above can also be used to investigate multicritical behavior (Griffiths, 1970; Fisher, 1974a). Such studies are usually complicated by the fact that the multicritical point must be located in a two-dimensional parameter space, and this process often involves an iterative procedure. In addition there are usually additional critical eigenvalue exponents due to the presence of additional scaling fields for the multicritical point. This process has been carried out quite carefully by Landau and Swendsen (1986) for the two-dimensional Blume–Capel ferromagnet and for the two-dimensional Ising antiferromagnet with next-nearest neighbor interactions in a magnetic field. Mean field predicts that for certain values of the interactions there is a tricritical point on the phase boundary whereas beyond a certain value the tricritical point is decomposed into a double critical point and a critical endpoint. The MCRG study showed that for quite a wide range of couplings below the predicted critical value there was only an ordinary tricritical point with no indication of the predicted change. The numerical estimates obtained for both the dominant and sub-dominant eigenvalue exponents also remained unchanged with modifications in the couplings and were in good agreement with the predicted values for an ordinary tricritical point. This study strongly suggests that the fluctuations in the two-dimensional model destroy the mean-field behavior and retain the normal tricritical behavior.

9.3.5 Dynamic problems: matching time-dependent correlation functions

The ideas described above can be extended to the consideration of time-dependent properties. The general idea behind this approach is to generate a sequence of states which have been blocked at different levels and compute the correlation functions as functions of time. Then attempt to 'match' these correlation functions at different blocking levels at different times. The relationship between the blocking level and the time at which they match gives the dynamic exponent z. Mathematically this can be expressed by

$$C(N, m, T_2, t) = C(Nb^d, m + 1, T_1, b^z t), \tag{9.28}$$

where the critical temperature is given by $T_1 = T_2 = T_c$. It is necessary to use two different size lattices for the comparison so that there are the same number of spins in the large lattice after the blocking as in the smaller lattice with one less blocking. Of course, we expect that the matching can be carried

out successfully only for some sufficiently large value of m for which the effect of irrelevant variables has become small. This approach was first implemented by Tobochnik *et al*. (1981) for simple one- and two-dimensional Ising models. For best results multiple lattice sizes should be used so that finite size effects can be determined and the procedure should be repeated for different times to insure that the asymptotic, long time behavior is really being probed (Katz *et al*., 1982).

9.3.6 Inverse Monte Carlo renormalization group transformations

The renormalization group approach is generally thought to be a semi-group because it has no unique inverse. Nonetheless, there have been several attempts made to implement a kind of inverse MCRG method for critical phenomena. Brandt and Ron (2001) introduced a renormalization multigrid method that used 'coarse to fine' acceleration. This approach relied upon knowledge of the renormalized Hamiltonian and was thus limited by the difficulty of estimating it. Ron *et al*. (2002) then devised a computationally stable inverse Monte Carlo renormalization group transformation that was built upon the renormalization group method and could simulate the fixed point of a renormalization group for large systems without critical slowing down. Using a seven-coupling Hamiltonian, as defined in Eqn. (9.19), they were able to compute the ratio γ/ν for the two-dimensional Ising model to an accuracy of 0.005%. In three dimensions the deviation was larger but was still quite good. One striking feature of this approach is that corrections to scaling were not visible, even on lattices as small as 4^2 and 4^3.

REFERENCES

Brandt, A. and Ron, D. (2001), *J. Stat. Phys*. **102**, 231.

Brezin, E., LeGuillou, J. C., Zinn-Justin, J., and Nickel, B. G. (1973), *Phys. Lett*. **44A**, 227.

Domb, C. and Green, M. S. (eds.) (1976), *Phase Transitions and Critical Phenomena*, vol. 6 (Academic Press, London).

Fisher, M. E. (1974a), *Rev. Mod. Phys*. **46**; 597.

Fisher, M. E. (1974b), *Phys. Rev. Lett*. **32**, 1350.

Friedman, Z. and Felsteiner, J. (1977), *Phys. Rev. B* **15**, 5317.

Griffiths, R. B. (1970), *Phys. Rev. Lett*. **24**, 715.

Guo, W., Blöte, H. W. J., and Ren, Z. (2005), *Phys. Rev. E* **71**, 046126.

Hsiao, P.-Y. and Monceau, P. (2003), *Phys. Rev. B* **67**, 064411.

Itakura, M. (2002), *J. Phys. Soc. Japan* **72**, 74.

Kadanoff, L. P. (1971), in *Critical Phenomena*, ed. M. S. Green (Academic Press, London).

Katz, S. L., Gunton, J. D., and Liu, C. P. (1982), *Phys. Rev. B* **25**, 6008.

Landau, D. P. and Swendsen, R. H. (1986), *Phys. Rev. B* **33**, 7700.

Lewis, A. L. (1977), *Phys. Rev. B* **16**; 1249.

Ma, S.-K. (1976), *Phys. Rev. Lett*. **37**, 461.

Nelson, D. R., Kosterlitz, J. M., and Fisher, M. E. (1974), *Phys. Rev. Lett*. **33**, 813.
Reynolds, P. J., Stanley, H. E., and Klein, W. (1980), *Phys. Rev. B* **21**, 1223.
Ron, D., Swendsen, R. H., and Brandt, A. (2002), *Phys. Rev. Lett*. **27**, 275701.
Swendsen, R. H. (1982), *Real Space Renormalization*, eds. T. W. Burkhardt and J. M. J. van Leeuwen (Springer Verlag, Heidelberg).
Tobochnik, J., Sarker, S., and Cordery, R. (1981), *Phys. Rev. Lett*. **46**, 1417.
Wegner, F. J. and Riedel, E. K. (1973), *Phys. Rev. B* **7**, 248.
Wilson, K. G. (1971), *Phys. Rev. B* **4**, 3174, 3184.
Wilson, K. G. and Fisher, M. E. (1972), *Phys. Rev. Lett*. **28**, 248.
Zinn-Justin, J. and Le Guillou, J. C. (1980), *Phys. Rev. B* **27**, 3976.